

DOI: <https://dx.doi.org/10.21123/bsj.2022.6782>

Breast Cancer MRI Classification Based on Fractional Entropy Image Enhancement and Deep Feature Extraction

Ali M. Hasan^{1*} 

Asaad F. Qasim² 

Hamid A. Jalab³ 

Rabha W. Ibrahim⁴ 

¹College of Medicine, Al-Nahrain University, Baghdad, Iraq.

²Ministry of Higher Education and Scientific Research, Studies, Planning and Follow-up Directorate, Baghdad, Iraq.

³Faculty of Computer Science and Information Technology, University of Malaya, 50603 Kuala Lumpur, Malaysia.

⁴ Faculty of Mathematics and Statistics, Ton Duc Thang University, Ho Chi Minh City 758307, Vietnam.

*Corresponding author: a.hasan4@colmed-alnahrain.edu.iq

E-mail addresses: A.Qasim@edu.salford.ac.uk , hamidjalab@um.edu.my , rabhaibrahim@tdtu.edu.vn

Received 23/11/2021, Revised 28/2/2022, Accepted 2/3/2022, Published Online First 20/7/2022,
Published 1/2/2023



This work is licensed under a [Creative Commons Attribution 4.0 International License](https://creativecommons.org/licenses/by/4.0/).

Abstract:

Disease diagnosis with computer-aided methods has been extensively studied and applied in diagnosing and monitoring of several chronic diseases. Early detection and risk assessment of breast diseases based on clinical data is helpful for doctors to make early diagnosis and monitor the disease progression. The purpose of this study is to exploit the Convolutional Neural Network (CNN) in discriminating breast MRI scans into pathological and healthy. In this study, a fully automated and efficient deep features extraction algorithm that exploits the spatial information obtained from both T2W-TSE and STIR MRI sequences to discriminate between pathological and healthy breast MRI scans. The breast MRI scans are preprocessed prior to the feature extraction step to enhance and preserve the fine details of the breast MRI scans boundaries by using fractional integral entropy FIE algorithm, to reduce the effects of the intensity variations between MRI slices, and finally to separate the right and left breast regions by exploiting the symmetry information. The obtained features are classified using a long short-term memory (LSTM) neural network classifier. Subsequently, all extracted features significantly improves the performance of the LSTM network to precisely discriminate between pathological and healthy cases. The maximum achieved accuracy for classifying the collected dataset comprising 326 T2W-TSE images and 326 STIR images is 98.77%. The experimental results demonstrate that FIE enhancement method improve the performance of CNN in classifying breast MRI scans. The proposed model appears to be efficient and might represent a useful diagnostic tool in the evaluation of MRI breast scans.

Keywords: Breast MRI scans, Classification, CNN, Deep features, LSTM.

Introduction:

According to the American Institute for Cancer Research, breast cancer is the most commonly occurring cancer and the second most common cancer among women in 140 of 148 countries worldwide. It is the main and second leading cause of cancer death in less developed countries and United States of America (USA) respectively. Since 2008, the number of registered breast cancer cases and the rate of mortality have increased significantly by 20% and 14% respectively ¹. Many breast cancer symptoms are invisible and not noticeable without a professional screening, but some symptoms can be caught early

just by being proactive about your breast health. According to the American Cancer Society, when breast cancer is detected and localized early, the 5-year relative survival rate is 99%. Early detection includes doing monthly breast self-exams and scheduling regular clinical breast exams plays an important role in the treatment and control of the disease ^{2,3}.

Breast lesion investigations may include self or clinical breast examination, in addition to a variety of other efficient complementary imaging techniques which provides additional details to achieve a definite breast diagnosis such as X-ray

Mammography, Ultrasonography (US) and Magnetic Resonance Imaging (MRI). Self-examination or also known by physical exam of breast by women themselves or by clinician, is current mainstays and the primary diagnostic choice for breast cancer detection that is contributed to the detection of any smaller unusual lumps. However, it remains controversial due to inherent limitations including the lack of standardization and the experience level of the examiner, variations in the definition of outline and in the texture of the cancer, variations in the texture of the normal surrounding breast tissue and biologic variations in the threshold size of a cancer before distant metastases occur⁴. Mammography is a low energy X-ray examination of the soft tissue of the breast. It measures the variation in density between normal breast features and pathological tissue texture to produce the mammographic images. These images are used to evaluate and assess the entire breast as well as characteristics, size and location of the suspicious area in the breast⁵. However, the utilization of mammography may increase the probability of cell damage and change the base of DNA due to expose radiation in a high sensitive tissue such as the breast^{6, 7}. Where, some studies have proved that the radiation of mammography may increase the incidence of breast cancer⁸. Additionally, many small lesions that are detected by physical exam, sometime are occulted by mammography. Additionally, the mammograms images of women with dense breast tissue, are particularly difficult to interpret especially in young women. Therefore, in clinical routine, once a breast cancer is detected by screening mammography or by physical exam, complementary imaging modalities are required to provide additional diagnostic information, achieve a high confidence and accurate diagnostic decision⁸. Over the last two decades, US and MRI have emerged as potential investigations for the detection and diagnosis of breast cancer⁵. US is a noninvasive imaging technology, uses high frequency acoustic waves that reflect at boundaries with different acoustic properties. It provides diagnostic details on both palpable and nonpalpable pathological breast. However, it has also number of limitations that associate with the overlapping in sonographic characteristics such as failure in discriminating both micro and macro calcifications in ductal carcinoma in situ (DCIS). Moreover, solid lesions especially in fatty breast could be missed and if detected, cannot determine whether a solid mass is benign or malignant^{5, 8}. MRI is a nonionizing and a highly sensitive tomographic functional technology that may be utilized effectively for screening pathological breast when

diagnosing with mammography is uncertain and increasing the number of screenings per year for patients at high risk for breast cancer^{5, 9}. MRI breast scan has an excellent soft tissue resolution that enhances the ability to identify the location and determine the full extent of the lesion. In addition, measuring the size of the cancer, look for other tumors in the breast and check for tumors in the opposite breast¹⁰. MRI uses a combination of a large magnet, radio-waves to excite tissues and a computer to produce high-resolution cross-sectional images of the organs and structures within the body. There are many different MRI sequences provide a valuable details information to discriminant pathological tissues with a spatial resolution up to 1×1×1 mm voxel size. MRI scanning starts with T2-weighted (T2W) sequences without contrast administration such as Fast Spin Echo (FSE), Turbo Spin Echo (TSE), Rapid Acquisition with Refocusing Echoes (RARE)¹¹. T2-weighted (T2W) scan provides much information to discriminant benign from malignant lesions based on determining bright signal. Where the lesions with higher water content appear as a hyperintense and more likely to be benign than malignant such as cysts, edema, intramammary lymph nodes, mucinous, fibroadenomas and necrotic breast tumors. While, some breast tumors appear as hypointense in T2W such as adenocarcinoma tumors¹⁰. Non-contrast T1-weighted (T1W) sequences is used routinely to evaluate normal anatomy due to images acquiring with high resolution and less artifact. In a typical breast MRI acquisition protocol, T1W scan is performed after administration of a contrast agent to the patient to enhance lesions. Subsequently, several postcontrast T1W scans that visualize lesions which do not appeared in pre-contrast MRI scan. These postcontrast scans provide essential information for distinguishing benign from malignant tumors⁹.

In breast anatomy, it consists of a set of respective proportions of tissues; fibrous tissue which is responsible to hold the entire breast tissues in their place. Glandular tissue which is also called lobe is the part of the breast that is responsible to make milk. The tubes that are also named ducts, are responsible to carry milk to the nipple. Finally, fatty tissue that fill the space between the fibrous tissue, lobes and ducts, these compositions of the breast could vary from patient to patient and give the breast size and shape as demonstrated in Fig. 1¹². It was evaluated that the percentage of fat volume to the overall breast volume varies between (7%-56%)¹³. As fat tissues have a short relaxation time in both T1W and T2W sequences, they appear as a hyperintense in both sequences. Therefore, if the fat

high signal intensity is not suppressed, the features of interest could be hidden and difficult to be distinguished from other tissues. Additionally, utilization of silicone as breast implants for breast surgery which is implanted under the breast tissue to either increase breast size or help to reconstruct the breast. Due to the silicone and fat have resonance frequencies are very closed to each other, the silicone appears as a hyperintense in T2W sequences. Therefore, the fat and silicone suppressions are necessary or highly desirable in different breast

sequences and usually achieved with inversion-recovery with short inversion time (STIR) sequence¹⁴. The STIR sequence is designed to suppress signal from fat and silicone as well as enhances the signal from tissue with long T1 and T2 relaxation times, such as neoplastic and inflammatory tissue. The turbo spin echo sequence (TSE) is another fundamental capability pulse sequence in MRI imaging that is used in many of clinical applications. It facilitates the fundamental contrasts of T2W and T1W by acquiring of images with low sensitivity to susceptibility and inhomogeneity effects. Most of breast pathologies which include high water content, appear as a hyperintense relative to the fat that appears as a hypointense on T2W-TSE sequences¹⁵.

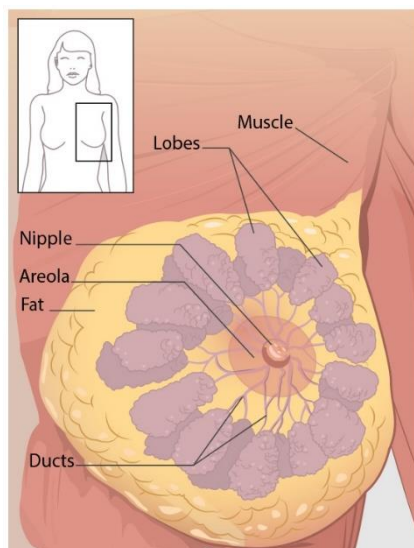


Figure 1: Breast anatomy¹².

Texture analysis is an essential integrated part in medical imaging techniques that allows to assess quantitatively and objectively of tissue heterogeneity by determining how the voxels are distributed⁴. It is an efficient way to extract high-level of features due to high sensitivity to the variations of grey-level intensities in medical images. It is indispensable tool in neuro-MR imaging and may be used as an alternative

diagnostic tool for MR image analysis after applying to machine learning¹⁶.

In this study, the diagnostic performance of convolutional neural networks (CNN) when used as feature extractor is investigated to discriminate normal and pathological tissues in breast MRI scans. The novelty of the proposed algorithm can be summarized as follows:

1. The model improves the performance of the breast cancer MRI classification by proposed a new fractional integral entropy (FIE) for image enhancement.
2. The pre-processing stage used for separating the left and right breasts from the intermammary cleft point through the use of mirror symmetry via registration (MSR) method.
3. Two MRI sequences (T2W-TSE and STIR) are used as input sequences for the CNN to improve the extracted features.

As demonstrated by the experimental results later in this study, it is evident that the proposed model can accurately and efficiently classify the tested input images. Due to its performance, the model has the potential to help radiologists to reduce reading time and prevent reading errors since it is able to detect pathologies that were misinterpreted or overlooked by radiologists during breast MRI screening. The rest of the paper is organized as follows: some recent related works are reviewed in Section 2. In Section 3, full description of the proposed model is presented. The detailed experimental consequences are investigated and discussed in Section 4, and lastly, Section 5 indicates the conclusions of the study.

Related Works

Recently, deep learning algorithms have established a notable presence in computer vision and image analysis^{16, 17}. Various studies have utilized deep learning algorithms for the detection and classification of breast cancer. For example, Jiang, et al.¹⁸ presented a model based on a number of SE-ResNet modules for the detection of breast tumors. The method consists of a convolutional layer as the first stage, a small SE-ResNet model as the second stage, and a fully connected layer as the third stage. The author reported a rather good detection efficiency with less parameters when evaluated using the BreakHis public database for automatic binary and multiclass classification. However, better detection results require setting up many parameters. The study by Dabeer, et al.¹⁹ presented a CNN based model to extract features from breast histopathological images and subsequently distinguish benign from malignant

tissues with the help of a classifier network. This method has reportedly achieved 99.86% prediction accuracy using the BreakHis dataset. However, the model depends on a sequence architecture design for the classification problem, and many parameters need to be set up prior to execution. The overfitting of the model on a small training set could have occurred.

In contrast to the aforementioned models, some other studies have proposed better-performing, yet less complex algorithms. For instance, Xiang, et al.²⁰ proposed a CNN as a feature extractor to discriminate images of breast cancer. The method was run against the BreakHis dataset, and showed an accuracy of 93.2%. However, as a drawback of this model, the architecture parameters of the CNN were initially fine-tuned for the histopathological images. Khan, et al.²¹ have proposed a transfer learning method to classify and detect breast cancer in images. Residual Networks, GoogleNet, and Visual Geometry Group Network were used to extract the features. The use of the transfer learning method constitutes the main advantage of this method since it improves the classification accuracy and accelerates the learning process. However, the pre-processing, feature selection, and extraction tasks have a complex nature, which can easily degrade the classification performance. Similarly, another algorithm which employs a hybrid technique of different deep networks for breast cancer histopathological images classification has been described in²². The features in this algorithm are only extracted from certain segmented parts of the image, while ignoring the background. This approach reportedly achieved an accuracy of 91.3% when tested on 4-breast cancer classification classes.

In the view of using deep learning as a powerful feature extraction tool, Lu 2019²³ proposed a new approach to enhance the detection and classification of tumor by merging MRI features and image information. The proposed model uses four different images as input and accordingly produces four types of feature maps as CNN output. Despite its potential, this technique increases the complexity of the proposed CNN model. Similarly, Yurttakal, et al.²⁴ used the pixel information of the MRI images alone in a CNN to classify lesions as malignant or benign. Even though the reported accuracy was 98.33%, this approach does not seem to be robust against system noise because it depends on the pixel information alone. More recently, deep learning approaches utilizing masked region based convolutional neural networks (R-CNN) have been proposed to detect potential lesions in breast MRI images^{25, 26}. The pre-processing step used in this

approach improves the classification accuracy. However, the masking approach may sometimes display overlapping errors and generate false edges which can degrade the overall accuracy. Lahoura, Singh²⁷ proposed a breast cancer detection system using a cloud environment. The proposed system exploited the potential capability of extreme learning machine (ELM) as a classification algorithm combined with the gain ration method to select the most prominence attributes. The experimental results indicated that the achieved accuracy was 98.6% on the WBCD dataset. From previous studies, some noteworthy facts used as inspiration are as follows:

1. Most of the studies did not enhance breast MRI scans primarily to reduce common artifacts that can have an effect on breast MRI scan.
2. The most important issue is that the previous studies did not consider that the breast cancer may be present in only one breast, and each breast must be evaluated and diagnosed separately.

Materials and Methods:

The proposed model utilizes deep neural network to extract features from T2W TSE and STIR MRI sequences which represent the preferred choice of clinicians to use and subsequently the long short-term memory (LSTM) to classify the images into either normal or pathological. The process includes three main stages: the pre-processing of the scans, the deep features (DF) extraction, and finally the LSTM network classifier. The proposed model is shown in Fig. 2.

- Dataset

A dataset comprising 89 breast MRI scans with confirmed diagnostic reports was downloaded from The Cancer Imaging Archive (TCIA)²⁸, of which 11 scans were of healthy patients and 78 were of pathological patients with different abnormalities such as high-risk normal, ductal carcinoma in situ, fibroids and carcinomas. Each scan comprised T2W and STIR sequences that were acquired by "PHILIPS Achieva 1.5 Tesla scanner". The 182 MRI cases were split into individual MRI images, and each image was separated into left and right breasts. Overall, 326 T2W-TSE images and 326 STIR images were obtained. Both MRI sequences (T2W-TSE and STIR) comprised 161 and 165 healthy and pathological images respectively. Figure 3 shows sample breast MRI images from the dataset. 80% of the 186 images were used to train the CNN and LSTM networks, while the remainder ("unseen") was used to test the model.

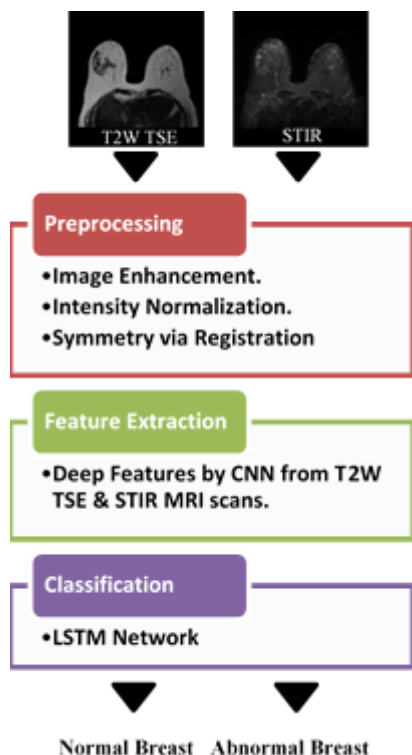


Figure 2. The Proposed Model of Breast MRI scans Classification.

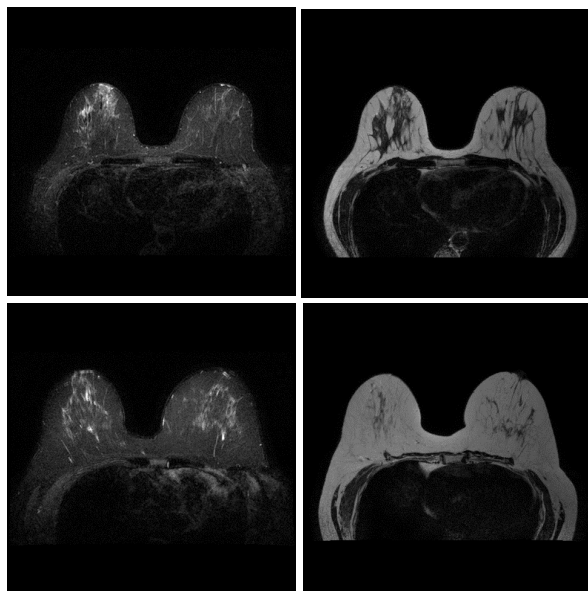


Figure 3. Samples of STIR and T2W-TSE scans. The first row shows healthy breasts while the second shows pathological breast.

- Breast MRI Image Preprocessing

Prior to the processing of the breast MRI images, a set of common pre-processing methods is used to reduce the artifacts that cause fluctuations in the intensity of the MRI scans. These artifacts can occur across the repeated scans, between different anatomic regions, or when acquiring the MRI scans from different scanners even though they use the

same acquisition protocol. The artifacts can be classified into three main groups: physiological artifacts, which are caused by patient movement, such as breathing, heartbeat and blood flow; artifacts that may rise from inherited physics of the MRI machine, such as metallic implants, foreign bodies or chemical shift; and finally, the artifacts that may come from hardware and/or software malfunctions. Therefore, preprocessing algorithms are needed to improve the quality of the MRI such as image enhancement and histogram normalization.

Inspired by the fact that fractional integral has the ability to find solutions to complex problems like non-linear complexities, a new fractional integral entropy FIE is explored to enhance and preserve the fine details of the breast MRI scans boundaries. The fractional integral (local fractional integral) is one of the significant approaches of fractional analysis, which is utilized to measure the fractional structures of data, such as images. Inspired by the methods²⁹⁻³¹ where fractional calculus has been explored, the FIE model is proposed for enhancing the image to improve the classification process. For each pixel in the image, the proposed model derives the fractional entropy based on pixels' probability to extract the image gray-level changes³²⁻³⁴.

For a dynamic function P and a variable u in $[a, b]$, the definition of fractional integral is given as follows³⁵.

$$I^{(q)} P(u) = \frac{1}{\Gamma(1+q)} \int_a^b P(u) (du)^q \quad 1$$

where Γ is Euler gamma function with the fractional power operator q . Recently, fractional entropies have been proposed by many researchers for solving fractional non-linear problems. Tsallis entropy as image enhancement algorithm is considered. The Tsallis entropy is defined as:

$$E_q(P(u)) = \frac{\int_a^b (P(u))^q du - 1}{1 - q} \quad 2$$

By using Eq. 1 for the function $(P(u))$, Eq. 3 is obtained

$$E_q^{(q)}(P(u)) = \frac{\int_a^b (P(u))^q du^q - 1}{(1 - q)\Gamma(1 - q)} \quad 3$$

In the discrete 2-D image format, Eq. 3 becomes:

$$E_q^{(q)}(i, j) = \frac{1}{(1 - q)\Gamma(1 - q)} \left(\sum_{j=1}^m \sum_{i=1}^n P^q(i, j) - 1 \right) \quad 4$$

where m and n are the image dimension, and the fractional parameter q .

The steps of the proposed model are as follow:

1. Set the quantum parameter $q = 0.3$
2. Calculate the image intensity occurrences number.

3. Calculate the probability of each intensity occurrences number.
 4. Calculate the sum of all pixels' probability P .
 5. Calculate the enhanced image by using Eq. 4.
- The output of the proposed FIE for a sample low contrast image is illustrated in Fig. 3. The details of the input images in Fig. 4 (a, b, and c), become brighter after the enhancement by proposed FIE

algorithm as shown in Fig. 3 (d, e, and f). The enhancement of the low visibility regions in the input images is due to the robust ability of FIE algorithm to deal with the dark image pixels in input images. The logic behind using FIE in image breast MRI enhancement is the capability of FIE to capture the image fine details efficiently.

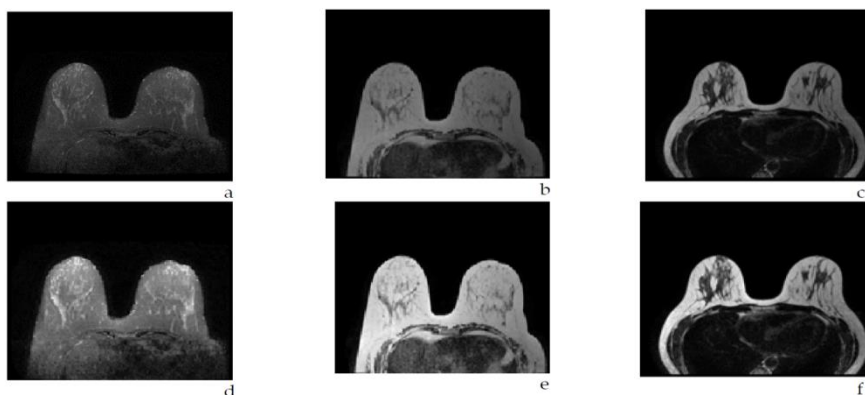


Figure 4. Sample breast MRI (STIR and T2W TSE scans) from the dataset. (a, b and c) Original 242 MRI images, (d, e and f) enhanced MRI images by proposed image enhancement.

Additional processing steps are carried out as well, including histogram normalization to reduce the artifacts that cause random fluctuations in the distribution of the intensity of the MRI scans. Where, these artifacts can occur across the repeated scans, between different anatomic regions, or when acquiring the MRI scans from different scanners even though they use the same acquisition protocol. In addition, identification of the breasts' boundaries, the removal of other chest parts, and the isolation of the background by thresholding the intensity values of each MRI slice individually. These steps are followed by a morphological operation to eliminate any generated holes in the segmented slice. Finally, a cleanup of the segmentation process is done to eliminate the small objects by using a binary mask of zeros and ones which represent the background and foreground respectively³³. Since breast cancer may be present in only one breast, each breast must be evaluated and diagnosed separately. "Detecting mirror symmetry via registration" (MSR) or also known as "reflection symmetry via registration" is used to find a fitting plane of mirror in the breast MRI slice in an axial view that separates left and right breast individually. The MSR mechanism of action is based on finding a reflection plane of the breast MRI slice, then registering the original and reflected breast MRI slices, and calculating the eigenvector of the first eigenvalue for the transformation matrix that represents the reflection and registration mappings. MSR is supported by random sample consensus of an ensemble of

normalized cross-correlation matches^{15, 36}. By considering the general shape of the breast and chest MRI slice in axial viewing, an ellipse model is used to fit the chest contour and cover all abdominal area roughly. Since the breast region can appear in various positions and orientations, the fitted ellipse is made to have a low eccentricity bias and affine invariance, and can be written as follows:

$$\frac{x^2}{A^2} + \frac{y^2}{B^2} = 1, \quad (A > B) \quad (5)$$

where, x and y are the points coordinates on the ellipse. A denotes the coordinate of the end points on the major axis which are also known as vertices, while B represents the coordinate of the end points on the minor axis which are also known as co-vertices. B should always be less than A in order to draw vertical ellipse. B is matched with the intermammary cleft region that is recognized by the MSR method. A is equal to the half of the width of the breast MRI slice. Figure 5 shows an example of a drawn vertical ellipse on a breast MRI slice. After drawing the vertical ellipse, all pixels inside the ellipse are set to zeros. The ones from the binary mask represent the breast region while the zeros represent the background. This mask is multiplied with the original MRI scan to extract the breast region alone. Finally, the breasts are separated into left and right sides from the intermammary cleft point after being recognized by the MSR method. The pseudo-code for the preprocessing step is shown in Algorithm 1. Figure 6 shows a sample of how a breast MRI slice is segmented and separated.

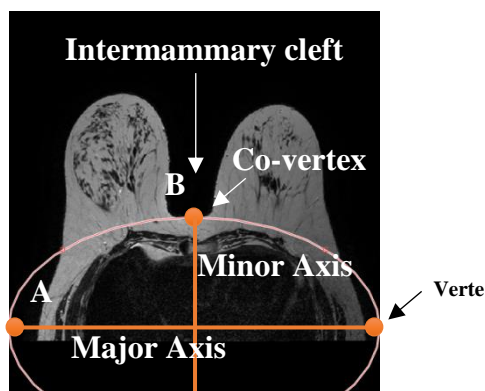


Figure 5. How the vertical ellipse is drawn on a breast MRI slice.

Algorithm 1. Pseudo-code for breast MRI scans preprocessing.

```

Input: Input breast MRI slice I(n,m)
Output: Output images Left and Right
Begin
  Adjust the value of pixels' intensity
  Convert into a binary image
  Fill image regions and holes
  Determine the intermammary cleft (B point) by MSR method.
  Draw the vertical ellipse to eliminate chest and abdominal area
  from the binary image
  Produce the output images L and R
  Multiply input image (I) by the binary image (BW) and separate
  the breast into left (L) and right (R) images from inter-mammary
  cleft point.
End
    
```

- Deep Image Feature Extraction

Even though the handcrafted feature methods are designed based on expert knowledge, they include many limitations¹⁶. Therefore, to efficiently extract more features for breast cancer classification, a learning-based technique is used to learn more features, and more specifically by using a CNN method. Many previous studies have successfully applied CNN in many computer vision systems^{16, 33, 37}. The main structure of CNN comprises the following layers: the convolutional layer, the batch normalization layer, the rectified linear activation function (ReLU), the pooling layer, and the fully connected layer. The convolutional layer comprises several tensors of feature maps which are determined by independently convoluting a set of small parameterized convolutional filters, named kernels, to every layer by shifting from one position to another with step size named stride. Practically, strides of one and two pixels have been already proven to perform well¹⁶.

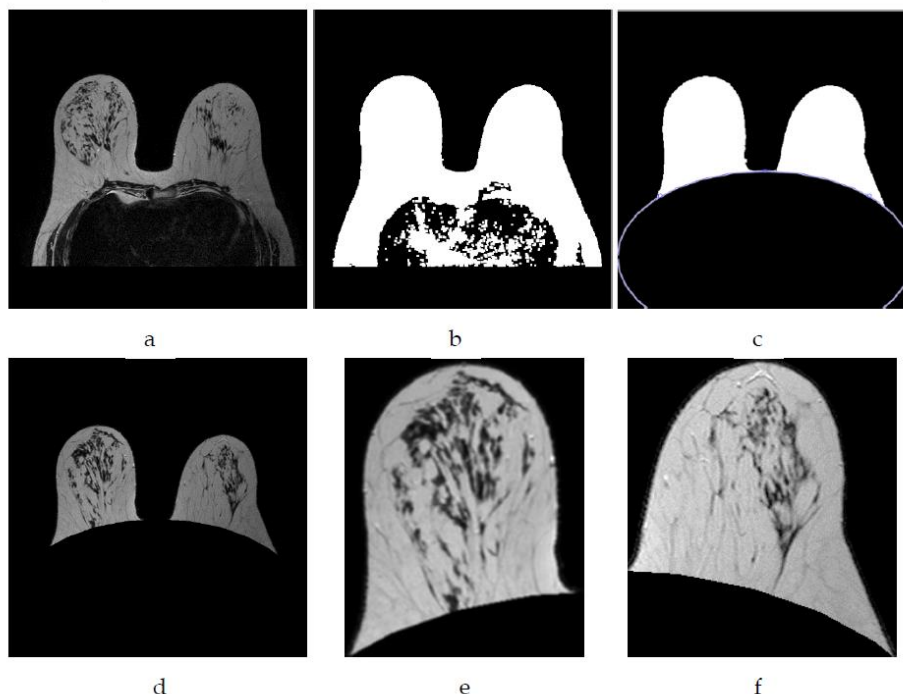


Figure 6. An example of breast MRI splitting, A) Original breast MRI slice, B) Segment the breast slice and create a mask, C) Eliminate the chest and abdominal areas from the mask by drawing an ellipse, D) Multiply the mask by the original MRI slice to extract the breast from it, Separated E) left and F) right breasts.

To ensure that all of the feature map is covered by the kernels, zero-padding is sometimes needed to pad the border of the feature map. All negative values in the feature maps are then

suppressed to zeros through rectified linear unit (ReLU) activation function in the activation layer. The resulting feature maps are normalized and regularized to avoid overfitting after each activation

layer through a batch normalization layer. The latter works as a regulator for the network and speeds up the training process. Then, the normalized feature maps are partitioned into small non-overlapped regions in the pooling layer and a single value is determined for each region. The feature extraction layer of CNN is the fully connected layer (FC). The main objective of the CNN in this study is to extract the high level of features for breast MRI scans classification. Because of architecting the CNN network is considered a big challenge and associated significantly with many hyperparameters that have a significant impact on the network efficiency such as depth of network (number of convolutional, pooling and fully connected layers), number of kernels, stride value, pooling function and number of units in the fully connected layer. Therefore, finding the proper hyperparameters

needs an expert knowledge and sometime as trial and error process. The proposed CNN is shown in Fig. 7.

The initial learning rate and epochs for training were set to 0.0001 and 40 respectively. The training continued until the loss in the validation set was stable. The utilized loss function during training was the log of the absolute value of the differences between the target and output likelihood values. The proposed CNN was initialized and optimized by using Xavier Glorot uniform and the stochastic gradient descent with momentum algorithms respectively. The network learnable parameters in a custom training loop were updated using the stochastic gradient descent (Adam) algorithm optimization. About 20% of the training dataset was separated at the patient level to be used as a validation set.

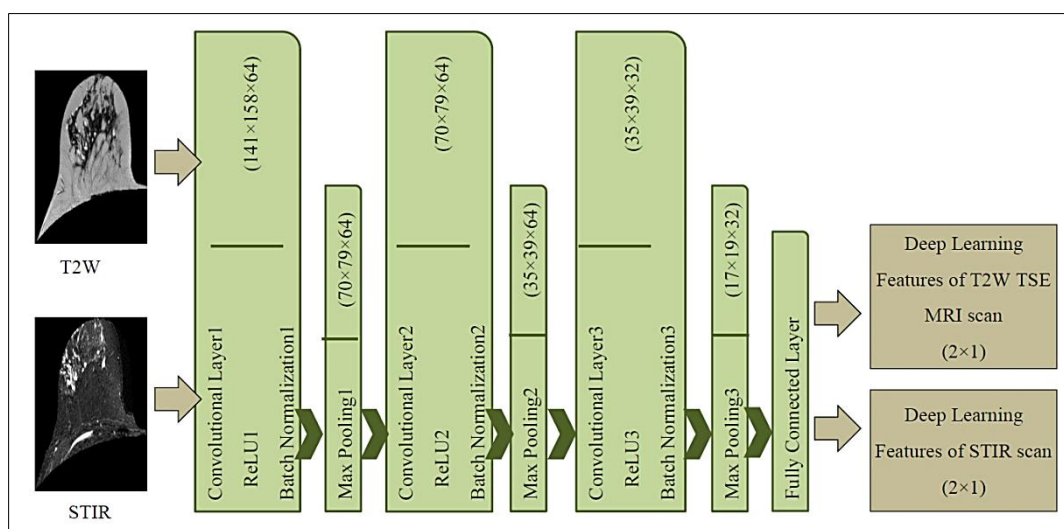


Figure 7. The architecture of proposed CNN as a deep feature extraction.

- LSTM Classifier

The LSTM is a recurrent neural network architecture which was originally proposed by Hochreiter and Schmidhuber to overcome the limitations of artificial neural networks and deal with the vanishing gradient problem that comes from a small vanishing of the gradient which effectively prevent the weight from changing its value. Resulting in stopping completely the neural network from further training¹⁷. It is capable of successfully learning data with long-term temporal dependencies, especially in sequence prediction problems due to the significant time lag between the input and its corresponding output. It is used to solve numerous tasks that are not solvable by other machine learning algorithms, such as language modeling, machine translation and handwriting recognition³⁸. Its learning ability comes from its internal cell state that works as a memory cell.

Three internal sigmoidal gates regulate the information within the network: the input gate i^t , the output gate o^t , and the forget gate f^t . Although, the LSTM is used for sequential data, but it can be used as a classifier due to its ability to recognize image features across time by the connected memory blocks through its layers. Where, it can be considered the time series in the mathematical expression of LSTM refers to the length of the input sequence^{16, 17, 33}. In this study, the extracted deep features from the two modalities of breast MRI scans can be considered as a time series. The LSTM network comprises six interacting layers; classic LSTM with 50 hidden units, dropout by 20%, classic LSTM with 200 hidden units, dropout by 20%, bidirectional LSTM with 400 hidden units and fully connected (FC) layers. Sequence input with 4 dimensions that comes from combined extracted features of T2W TSE and STIR modalities of breast

MRI scans. The LSTM network was trained by using Adam optimization method. The maximum epoch value and the gradient threshold value were set to 100 and 1 respectively.

Experimental Results:

The experiments demonstrate the effectiveness of the extracted features that are used to classify the breast MRI scans into normal and abnormal scans. The proposed model is tested on two modalities of MRI scans (T2W TSE and STIR scans), which represent the preferred choice for the clinicians to diagnose, show the pathologic conditions and analyze the breast MRI scans. The collected dataset is partitioned into 80% for training the CNN, and 20% for testing as unseen breast MRI scans. Although, the MRI is considered as indispensable imaging technology that currently offers the most sensitive non-invasive way to visualize and understand much more about the underlying pathology of the disease. But there are several factors that affect the quality of MRI images such as the variations and random fluctuations in the intensity. These factors occur across the repeated scans, between different anatomic regions, or acquiring MRI scans from different scanners even though they use the same acquisition protocol. These may affect the diagnosing process significantly³⁹. Therefore, all the breast MRI scans were enhanced by FIE method and normalized by histogram normalization method in the preprocessing stage.

The proposed CNN composes eight layers as summarized in Table 1: an input layer, three convolutional layers, three max pooling layers, and one fully connected layer. To reduce the complexity of all CNNs, shorten the training time, and combat overfitting, a stride value of 2 was used for all layers, and the features map was down sampled independently after each pooling. The width and height of the features maps were reduced by a value equal to the original stride value, but with the depth remaining intact. The learning rate, batch size, momentum, and weight decay of the proposed CNN network were fixed to enable the convergence of the loss function in the training process to be in a balance between underfitting and overfitting. Fig. 8 shows the training process of the proposed CNN network. The experiments are implemented on Intel i7-6700HQ CPU (2.6 GHz) 8 GB RAM, 64-bit Windows 10, NVIDIA GTX 950 GPU, MATLAB 2020a.

Table 1. The details of the CNN layers of the proposed model

| Layer Name | Kernel Size | Feature Map |
|---------------------|-------------|--------------|
| Input layer | (141×158) | |
| Convolution layer 1 | (3×3) | (141×158×64) |
| Max. Pooling1 | (2×2) | (70×79×64) |
| Convolution layer 2 | (3×3) | (70×79×64) |
| Max. Pooling2 | (2×2) | (35×39×64) |
| Convolution layer 3 | (3×3) | (35×39×64) |
| Convolution layer 4 | (3×3) | (35×39×32) |
| Convolution layer 5 | (7×7) | (35×39×32) |
| Max. Pooling5 | (2×2) | (17×19×32) |
| Fully Connected | (1×2) | (1×2) |

The classification results were validated by considering the true negative (TN), true positive (TP), and accuracy as primary performance metrics. The TN and TP refer to the number of healthy and pathological breast MRI scans respectively that are correctly classified as such by the LSTM. The effect of the proposed FIE method on the performance of CNN model is evaluated by comparing TP and TN values of the two groups with the performance of CNN when using it individually as demonstrated in Table 2. Fig. 9 shows how the performance of CNN with FIE enhancement outperforms its performance when using deep features individually.

For comparative analysis, the performance of the proposed model was compared with the performance of three pre-trained networks⁴⁰⁻⁴² when tested on the same dataset. The results of the comparative analysis are presented in Table 3. It can be seen that the proposed model performs better than the existing methods in terms of the given metrics.

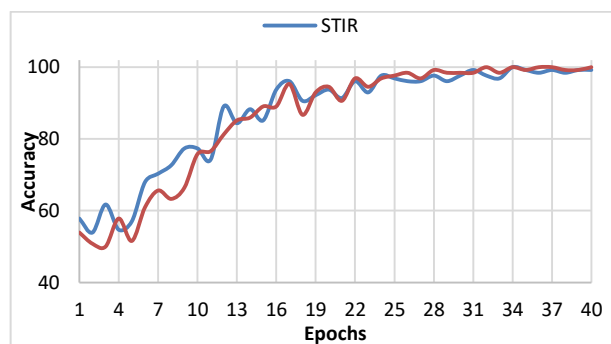


Figure 8. Training process of the proposed model.

Table 2. Comparisons of deep features of breast MRI scans with and without FIE.

| MRI modality | | TP | TN | Accuracy |
|--------------|----------------|--------|--------|----------|
| | | 100% | 100% | 100% |
| Without FIE | T2W TSE | 95.7% | 96.9% | 96.3% |
| | STIR | 96.3% | 97.5% | 96.9% |
| | T2W TSE & STIR | 97.5% | 98.1% | 97.8% |
| With FIE | T2W TSE | 96.9% | 97.5% | 97.20% |
| | STIR | 97.5% | 98.2% | 97.85% |
| | T2W TSE & STIR | 98.75% | 98.78% | 98.77% |

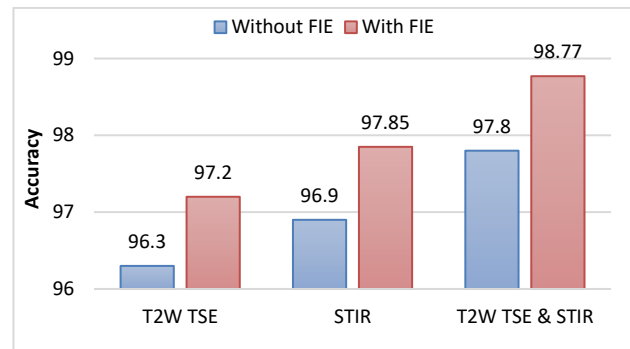


Figure 9. How the performance of deep features of breast MRI scans is improved with FIE enhancement.

Table 3. Comparisons between the proposed model and other pre-trained networks

| Method | No. of Layers | Feature Dimensions | TP 100% | TN 100% | Accuracy 100% |
|--------------------------|---------------|--------------------|---------|---------|---------------|
| AlexNet ⁴⁰ | 8 | 4096 | 92 | 90 | 90.50 |
| GoogleNet ⁴¹ | 144 | 1000 | 93.78 | 90.30 | 92.02 |
| SqueezeNet ⁴² | 18 | 1000 | 95.65 | 94.54 | 96 |
| Proposed CNN | 8 | 4 | 98.75 | 98.78 | 98.77 |

For comparison purposes, the following methods were used: Mai, Mao ⁴³ used six methods for feature extraction to extract 30 predictors from four MRI modalities (T2W, STIR, T1-weighted pre-contrast, and two contrast-enhanced series), then the extracted features were refined and analyzed by using Mann-Whitney and linear discriminant analysis respectively. Finally, the K-nearest neighbor classifier was used to classify the breast MRI scans. The achieved accuracy from classifying only 84 breast MRI cases was 95.2%. Yurttakal et al ²⁴ used a multi-layer CNN that included 28 deep layers as a feature extractor to discriminant breast tumorous regions. The proposed network achieved an accuracy of 98.33% when evaluated with 200 breast MRI images. Lu et al ²³ proposed an automated breast cancer classification technique that is based on merging four MRI modalities (T1W, T2W, diffusion weighted and dynamic contrast-enhancement (DCE)). These four modalities were passed into a CNN modal to extract four feature maps which were subsequently used to classify the breast MRI scans into either healthy or pathological. The achieved accuracy was 94.2% when tested with 67 breast MRI scans. Zhang et al ²⁵ used a deep learning mask regional convolutional

neural network (R-CNN) to recognize and segment the suspicious lesions in breast MRI scans. The achieved accuracy from segmenting breast MRI scans was 86%. The proposed method from the present study was compared with the above-mentioned methods in terms of the achieved accuracy and the number of breast MRI scans. As shown in Table 4, the proposed model achieved the highest score in both measures compared to the existing methods. In summary, the proposed model works well for the classification of breast MRI scans, and thus, has a good generalization capability to support the radiologists in the clinical setting.

The limitations of our study were the dynamic contrast-enhanced (DCE) MRI of the breast which is extremely sensitive in the detection of invasive breast cancer was not considered in this study. Where, the DCE may improve the performance of the proposed model in detecting non-mass lesions. Additionally, the two breasts have the same (mirrored) shapes is assumed to identify intermammary cleft point which is used to separate the breasts into left and right sides. While, this assumption holds for most of the cases, some patients may have asymmetric breast shapes.

Table 4. Comparisons between the proposed model and other methods

| Methods | Dataset | MRI Modality | Features | Accuracy 100% |
|-----------------------|---------|--|--|---------------|
| Mai, Mao [43] | 84 | - STIR - T1W - T1W | - Histogram - Absolute gradient - GLCM - GLRLM - Autoregressive Model - Wavelet | 95.20 |
| Yurttakal, Erbay [24] | 200 | - T1W - T2W | - CNN (28 Layers) | 98.33 |
| Lu, Wang [23] | 67 | - T1W - T2W - Diffusion weighted | - Vgg 16 - ResNet-50 - Inception V3 | 94.2 |
| Zhang, Chan [25] | 241 | - DCE - DCE | - DenseNet - Mask R-CNN - ResNet-101 | 86 |
| Proposed method | 326 | - STIR - T2W-TSE | - CNN (8 Layers) | 98.77 |

Conclusions:

In this study, a novel model is presented for an efficient and an accurate discrimination between pathological and healthy breast MRI scans. An extraction process of texture features that have the potential to support the diagnostic skills of radiologists was performed because they capture spatial and spectral frequency patterns, often not easily visible to the human reader. The proposed model achieves the desirable efficiency by separating the left and right breasts, which in turn improves the performance of the deep learning feature extraction by applying the proposed a new FIE image enhancement algorithm. As for accuracy, it is enhanced by using two MRI sequences (the T2W-TSE and STIR) as input sequences for the CNN, which overall improves the extracted features. The model has achieved an accuracy of 98.77% by the LSTM classifier for a dataset comprising breast MRI slices. Overall, the proposed model demonstrated highly desirable qualities for breast cancer classification from breast MRI scans, and could thus be considered for implementation in a clinical setting.

Future works comprise an implementation of extensive validation of the extracted deep learning features to detect non-mass lesions compared to high detecting rate of mass lesions. More training data of non-mass lesions and the development of dedicated algorithms may be needed to increase detection performance for such lesions.

Authors' declaration:

- Conflicts of Interest: None.
- We hereby confirm that all the Figures and Tables in the manuscript are mine ours. Besides, the Figures and images, which are not mine ours,

have been given the permission for re-publication attached with the manuscript.

- Authors sign on ethical consideration's approval
- Ethical Clearance: The project was approved by the local ethical committee in Al-Nahrain University.
- **Ethical Clearance:** This article does not contain any contact with human participants performed by any of the authors.

Authors' contributions statement:

Conception, design and drafting the manuscript, A.M.H.; acquisition of data and analysis, A. F. Q.; interpretation, revision and proofreading, H.A.J.; formal analysis, R.W.I. All authors have read and agreed to the published version of the manuscript.

References:

1. Breast cancer facts and figures 2019–2020. Am Cancer Soc: 1-44. Available from: <https://www.cancer.org/content/dam/cancer-org/research/cancer-facts-and-statistics/breast-cancer-facts-and-figures/breast-cancer-facts-and-figures-2019-2020.pdf>.
2. Smith R, Brawley O, Wender R. Screening and Early Detection, Principles of Oncology. Am Cancer Soc. 2018: 110-135. Available from: <https://doi.org/10.1002/9781119468868.ch11>.
3. AL-Thaweni A, Yousif W, Hassan S. Detection of BRCA1 and BRCA2 mutation for Breast Cancer in Sample of Iraqi Women above 40 Years. Baghdad Sci J. 2010; 7 (1): 394-400.
4. Marcon M, Ciritsis A, Rossi C, Becker A, Berger N, Wurnig M, et al. Diagnostic performance of machine learning applied to texture analysis-derived features for breast lesion characterisation at automated breast ultrasound: a pilot study. Eur Radiol Exp. 2019; 3(1): 44. Available from: <https://doi.org/10.1186/s41747-019-0121-6>.

5. Alnafea M. Detection and Diagnosis of Breast Diseases, in Breast Imaging. 2017, IntechOpen Book Series. Available from: <http://doi.org/10.5772/intechopen.69898>
6. Nahid A, Kong Y. Involvement of Machine Learning for Breast Cancer Image Classification: A Survey. *Comput Math Methods Med.* 2017; 2017:3781951. Available from: <https://doi.org/10.1155/2017/3781951>.
7. Hussain A, AL-Khafaji A, Ali A, Mohammed H. Study of Certain Biomarkers in Iraqi Female Patients with Breast Cancer. *Baghdad Sci J.* 2021; 18(4): 1140-1148. Available from: <https://doi.org/10.21123/bsj.2021.18.4.1140>.
8. Milosevic M, Jankovic D, Milenkovic A, Stojanov D, Early diagnosis and detection of breast cancer. *Technol Health Care.* 2018; 26(4): 729-759. Available from: <https://content.iospress.com/articles/technology-and-health-care/thc181277>
9. Dalmiş M, Vreemann S, Kooi T, Mann R, Karssemeijer N, Gubern A. Fully automated detection of breast cancer in screening MRI using convolutional neural networks. *J Med Imaging.* 2018; 5(1): 014502. Available from: <https://pubmed.ncbi.nlm.nih.gov/29340287/>.
10. Lin C, Rogers C, Majidi S. Fat suppression techniques in breast magnetic resonance imaging: a critical comparison and state of the art. *Rep Med.* 2015; 8: 37-49. Available from: <https://doi.org/10.2147/RMLS46800>
11. Kilic F, Ogul H, Bayraktutan U, Gumus H, Unal O, Kantarci M, et al. Diagnostic magnetic resonance imaging of the breast. *Eurasian J Emerg Med.* 2012; 44(2): 106. Available from: <https://www.eajm.org/en/diagnostic-magnetic-resonance-imaging-of-the-breast-132589>.
12. Jiménez-Gaona Y, Rodríguez-Álvarez M, Lakshminarayanan V. Deep-Learning-Based Computer-Aided Systems for Breast Cancer Imaging: A Critical Review. *Appl Sci.* 2020; 10(22): 8298. Available from: <https://doi.org/10.3390/app10228298>.
13. Vandeweyer E, Hertens D. Quantification of glands and fat in breast tissue: an experimental determination. *Ann Anat.* 2002; 184(2): 181-184. Available from: <https://www.sciencedirect.com/science/article/abs/pii/S0940960202800164?via%3Dihub>
14. Thomassin I, Trop I, Lalonde L, David J, Péloquin L, Chopier J. Tips and techniques in breast MRI. *Diagn Interv Imaging.* 2012; 93(11): 828-839. Available from: <https://pubmed.ncbi.nlm.nih.gov/23084072/>
15. Hilal S, Hasan H, Hasan A. Magnetic Resonance Imaging Breast Scan Classification based on Texture Features and Long Short-Term Memory Model. *Neuro Quantology,* 2021; 19(7): 41. Available from: <https://www.proquest.com/openview/fc40762cbf3d70d60719e0201b402264/1.pdf?pq-origsite=gscholar&cbl=2035897>.
16. Hasan A, Jalab H, Meziane F, Hasan K, Al-Ahmed A. Combining deep and handcrafted image features for MRI brain scan classification. *IEEE Access.* 2019; 7: 79959-79967. Available from: <https://ieeexplore.ieee.org/document/8736208>.
17. Hasan A, Jalab H, Ibrahim R, Meziane F, AL-Shamasneh A, Obaiys S. MRI brain classification using the quantum entropy LBP and deep-learning-based features. *Entropy.* 2020; 22(9): 1033. Available from: <https://doi.org/10.3390/e22091033>.
18. Jiang Y, Chen L, Zhang H, Xiao X. Breast cancer histopathological image classification using convolutional neural networks with small SE-ResNet module. *PloS one.* 2019; 14(3): e0214587. Available from: <https://doi.org/10.1371/journal.pone.0214587>.
19. Dabeer S, Khan M, Islam S. Cancer diagnosis in histopathological image: CNN based approach. *Inform Med Unlocked.* 2019; 16: 100231. Available from: <https://doi.org/10.1016/j.imu.2019.100231>.
20. Xiang Z, Ting Z, Weiyan F, Cong L. Breast Cancer Diagnosis from Histopathological Image based on Deep Learning. *Chin. Control Decis. Conf.* 2019. IEEE. China. Available from: <https://ieeexplore.ieee.org/document/8833431>.
21. Khan S, Islam N, Zahoor J, Din I, Rodrigues J. A novel deep learning based framework for the detection and classification of breast cancer using transfer learning. *Pattern Recognit. Lett.* 2019; 125: 1-6. Available from: <https://doi.org/10.1016/j.patrec.2019.03.022>.
22. Yan R, Ren F, Wang Z, Zhang T, Liu Y, Rao X, et al. Breast cancer histopathological image classification using a hybrid deep neural network. *Methods.* 2020; 173: 52-60. Available from: <https://doi.org/10.1016/j.jymeth.2019.06.014>.
23. Lu W, Wang Z, He Y, Yu H, Xiong N, Jianguo W. Breast Cancer Detection Based on Merging Four Modes Mri Using Convolutional Neural Networks. *Proc IEEE Int Conf Acoust Speech Signal Process.* 2019. IEEE. United Kingdom. Available from: <https://ieeexplore.ieee.org/document/8683149>.
24. Yurttakal A, Erbay H, İkiçeli T, Karaçavuş S. Detection of breast cancer via deep convolution neural networks using MRI images. *Multimed. Tools Appl.* 2020; 79: 15555-15573. Available from: <https://link.springer.com/article/10.1007/s11042-019-7479-6>.
25. Zhang Y, Chan S, Park V, Chang K, Mehta S, Kim M, et al. Automatic Detection and Segmentation of Breast Cancer on MRI Using Mask R-CNN Trained on Non-Fat-Sat Images and Tested on Fat-Sat Images. *Acad Radiol.* 2022; 29 Suppl 1(Suppl 1): S135-S144. Available from: <https://pubmed.ncbi.nlm.nih.gov/33317911/>.
26. Zebari D, Ibrahim D, Zeebaree D, Haron H, Salih M. Damaševićius R., et al., Systematic Review of Computing Approaches for Breast Cancer Detection Based Computer Aided Diagnosis Using Mammogram Images. *Appl Artif Intell.* 2021: 1-47. Available from: <https://doi.org/10.1080/08839514.2021.2001177>.
27. Lahoura V, Singh H, Aggarwal A, Sharma B, Mohammed M, Damaševićius R, et al. Cloud Computing-Based Framework for Breast Cancer

- Diagnosis Using Extreme Learning Machine. *Diagnostics*. 2021; 11(2): 241. Available from: <https://doi.org/10.3390/diagnostics11020241>.
28. Bloch B, Jain A, Jaffe C, Data From BREAST-DIAGNOSIS, T C I. *Archive*. 2020. Available from: <http://doi.org/10.7937/K9/TCIA.2015.SDNRQXXR>.
29. Jalab H, Ibrahim R. Fractional Alexander polynomials for image denoising. *Signal Process*. 2015; 107: 340-354. Available from: <https://doi.org/10.1016/j.sigpro.2014.06.004>.
30. Raghunandan K, Shivakumara P, Jalab H, Ibrahim R, Kumar G, Pal U, et al. Riesz fractional based model for enhancing license plate detection and recognition. *IEEE Trans Circuits Syst Video Technol*. 2017; 28(9): 2276-2288. Available from: <https://ieeexplore.ieee.org/document/7944571>.
31. Roy S, Shivakumara P, Jalab H, Ibrahim R, Pal U, Lu T. Fractional poisson enhancement model for text detection and recognition in video frames. *Pattern Recognit*. 2016; 52: 433-447. Available from: <https://doi.org/10.1016/j.patcog.2015.10.011>.
32. Ibrahim R, Moghaddasi Z, Jalab H, Rafidah N. Fractional differential texture descriptors based on the machado entropy for image splicing detection. *Entropy*. 2015; 17(7): 4775-4785. Available from: <https://doi.org/10.3390/e17074775>.
33. Hasan A, AL-Jawad M, Jalab H, Shaiba H, Ibrahim R, AL-Shamasneh A. Classification of Covid-19 Coronavirus, Pneumonia and Healthy Lungs in CT Scans Using Q-Deformed Entropy and Deep Learning Features. *Entropy*. 2020; 22(5): 517. Available from: <https://doi.org/10.3390/e22050517>.
34. Al-Shamasneh A, Jalab H, Palaiahnakote S, Obaidallah U, Ibrahim R, El-Melegy M. A new local fractional entropy-based model for kidney MRI image enhancement. *Entropy*. 2018; 20(5): 344. Available from: <https://doi.org/10.3390/e20050344>.
35. Yang X, Baleanu D, Srivastava H. *Local fractional integral transforms and their applications*. 2015, AP. 1st Edition, Elsevier. Available from: <https://doi.org/10.1016/B978-0-12-804002-7.09994-0>.
36. Cicconet M, Hildebrand D, Elliott H. Finding mirror symmetry via registration. *arXiv preprint arXiv: 2017; 1611.05971*. Available from: <https://arxiv.org/abs/1611.05971>.
37. Xia L, Xi S, Yongxia Z, Xiuhui W, Tie-Qiang L. Classification of breast cancer histopathological images using interleaved DenseNet with SENet (IDSNet). *PloS one*. 2020; 15(5): e0232127. Available from: <https://doi.org/10.1371/journal.pone.0232127>.
38. Le X, Ho H, Lee G, Jung S. Application of long short-term memory (LSTM) neural network for flood forecasting. *Water*. 2019; 11(7): 1387. Available from: <https://doi.org/10.3390/w11071387>.
39. Jalab H, Hasan A, Magnetic Resonance Imaging Segmentation Techniques of Brain Tumors: A Review. *Arch Neurosci*. 2019; 6(Brain Mapping): e84920. Available from: <https://brief.land/ans/articles/84920.html>.
40. Russakovsky O, Deng J, Su H, Krause J, Satheesh S, Ma S, et al. Imagenet large scale visual recognition challenge. *Int J Comput Vis*. 2015; 115(3): 211-252. Available from: <https://link.springer.com/article/10.1007/s11263-015-0816-y>.
41. Zhou B, Khosla A, Lapedriza A, Torralba A, Oliva A. An image database for deep scene understanding. *arXiv preprint arXiv: 2016; 1610.02055*. Available from: <https://arxiv.org/abs/1610.02055>.
42. Iandola F, Han S, Moskewicz M, Ashraf K, Dally W, Keutzer K. SqueezeNet: AlexNet-level accuracy with 50x fewer parameters and < 0.5 MB model size. *arXiv preprint arXiv: 2016; 1602.07360*. Available from: <https://arxiv.org/abs/1602.07360>.
43. Mai H, Mao Y, Dong T, Tan Y, Huang X, Wu S, et al. The utility of texture analysis based on breast magnetic resonance imaging in differentiating phyllodes tumors from fibroadenomas. *Front Oncol*. 2019; 9: 1021. Available from: <https://www.ncbi.nlm.nih.gov/pmc/articles/PMC6803552/>.

تصنيف صور الرنين المغناطيسي للثدي بالاعتماد على تحسين الصور واستخراج الخواص العميقة

رابحة وائل إبراهيم⁴

حامد عبدالله جلاب³

اسعد فليح قاسم²

علي مجيد حسن^{1*}

¹ جامعة النهرين، كلية الطب، بغداد، العراق.

² وزارة التعليم العالي والبحث العلمي، دائرة الدراسات والتخطيط والمتابعة، بغداد، العراق

³ كلية علوم الحاسبات وتكنولوجيا المعلومات، جامعة مالايا، كوالالمبور، ماليزيا

كلية الرياضيات والاحصاء، جامعة Ton Duc Thang، فيتنام

الخلاصة:

سرطان الثدي يعتبر واحد من الامراض الفاتلة الشائعة بين النساء في جميع أنحاء العالم. والتشخيص المبكر لسرطان الثدي الكشف المبكر من أهم استراتيجيات الوقاية الثانوية. نظرًا لاستخدام التصوير الطبي على نطاق واسع في تشخيص العديد من الأمراض المزمنة ومراقبتها، فقد تم اقتراح العديد من خوارزميات معالجة الصور على مر السنين لزيادة مجال التصوير الطبي بحيث تصبح عملية التشخيص أكثر دقة وكفاءة. تقدم هذه الدراسة خوارزمية جديدة لاستخراج الخواص العميقة من نوعين من صور الرنين المغناطيسي T2W-TSE و STIR MRI كمدخلات للشبكات العصبية العميقة المقترحة والتي تُستخدم لاستخراج الخواص للتمييز بين فحوصات التصوير بالرنين المغناطيسي للثدي المرضية والصحية. في هذه الخوارزمية، تتم معالجة فحوصات التصوير بالرنين المغناطيسي للثدي مسبقًا قبل خطوة استخراج الخواص لتقليل تأثيرات الاختلافات بين شرائح التصوير بالرنين المغناطيسي، وفصل الثدي الايمن عن الايسر، بالإضافة الى عزل خلفية الصور. وقد كانت أقصى دقة تم تحقيقها لتصنيف مجموعة بيانات تضم 326 شريحة تصوير بالرنين المغناطيسي للثدي 98.77%. يبدو أن النموذج يتسم بالكفاءة والأداء ويمكن بالتالي اعتباره مرشحًا للتطبيق في بيئة سريرية.

الكلمات المفتاحية: مسح الثدي بالرنين المغناطيسي، التصنيف، الشبكات العصبية الملتقة، الخواص العميقة، ذاكرة طويلة قصيرة الامد.